Journal of Materials Chemistry C

Accepted Manuscript

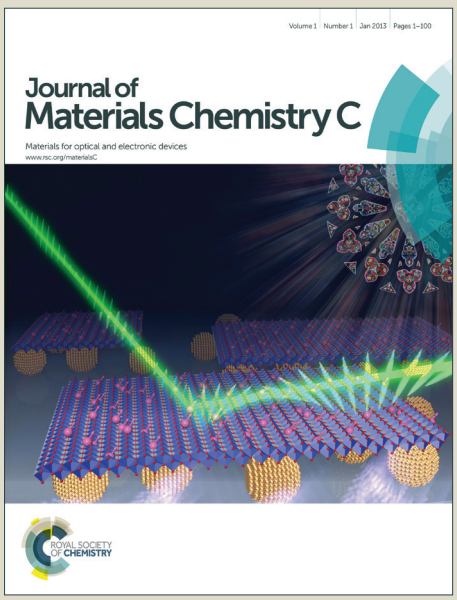

ROYAL SOCIETY OF CHEMISTRY

www.rsc.org/materialsC

Cite this: DOI: 10.1039/c0xx00000x

www.rsc.org/xxxxxx

ARTICLE TYPE

Power conversion efficiency enhancement in diketopyrrolopyrrole based solar cells through polymer fractionation

Iain Meager,[a] Raja Shahid Ashraf,[a] Christian B. Nielsen,[a] Jenny E. Donaghey,[a] Zhenggang Huang[a], Hugo Bronstein[b,] James R. Durrant[a] and Iain McCulloch.[a]

Received (in XXX, XXX) Xth XXXXXXXXX 20XX, Accepted Xth XXXXXXXXX 20XX
DOI: 10.1039/b000000x

Post polymerisation fractionation of diketopyrrolopyrrole based conjugated polymers through preparative gel permeation chromatography affords a varying range of molecular weight fractions with narrowed polydispersities. When used as the electron donor material in bulk heterojunction solar cells with both conventional and inverted architecture efficiency enhancements in excess of 50% are observed relative to non-fractionated material with the highest molecular weight fraction demonstrating a power conversion efficiency of 6.3%.

Introduction

Conjugated semiconducting polymers have great potential in a wide variety of organic electronic applications. In particular, the strive towards low cost organic photovoltaic (OPV) materials and devices receives much attention due to their ability to provide low cost renewable energy solutions.[123] When designing suitable polymeric materials a large synthetic effort is often focussed on structural design, in order to exert control over the optoelectronic properties.[456] There are however problems that are intrinsic to the use of polymers in electronic applications that can limit their reliability and reproducibility, both of which are essential if commercialisation is to be realised. Between any two polymer batches there can be large variations in molecular weight, polydispersity, homocouplings, defects and impurities amongst others.[78] Routes towards polymers of defined purity, molecular weight and polydispersity are therefore highly desirable and can lead to greater batch reproducibility and uniformity in a variety of intrinsic material properties which have been shown to be advantageous to OPV device performance parameters.[91011]

Diketopyrrolopyrrole (DPP) is a versatile and widely used structural motif in organic electronics comprising of an electron deficient core that is typically flanked by electron rich aromatic units. When incorporated into conjugated polymers this results in donor-acceptor type backbone structures with narrow optical band gaps as a result of molecular orbital hybridisation.[121314131516] We previously reported the introduction of thieno[3,2-*b*]thiophene as the flanking aromatic unit in DPP based copolymers and demonstrated its potential for high performance OPV applications with good bulk heterojunction power conversion efficiencies of 5.4%.[1718] Subsequent work showed that replacing the 2-octyl-1-dodecyl (C_8C_{10}) alkyl chain for a larger 2-decyl-1-tetradecyl ($C_{10}C_{12}$) facilitated improved polymer solubility which in turn allowed significantly higher molecular weight polymers and a wider range of copolymer structures to be accessed.[19] The highest performance in the $C_{10}C_{12}$DPPTT series was observed when thiophene was employed as a comonomer unit (figure 1.) giving an efficiency of 4.1%. Despite the improved molecular weight of the $C_{10}C_{12}$DPPTT-T material compared to its shorter chain analogue its efficiency was slightly lower and further work into maximising its potential was of interest.

Herein we report the post-polymerisation fractionation and purification of $C_{10}C_{12}$DPPTT-T by preparative gel permeation chromatography (GPC) to isolate polymer fractions of higher molecular weights and narrowed polydispersities. Purification by fractionation has previously been shown to be an effective technique for OPV performance enhancement in various polymer structures such as indacenodithiophene and it was hoped that a similar or greater improvement could be observed with the DPPTT-T backbone structure.[202122] Both conventional and inverted bulk heterojunction architectures show significant improvements in device performances with purified fractions demonstrating a range of power conversion efficiencies up to 6.3%. The unfractionated material and each purified fraction are analysed in both the neat polymer film and polymer : fullerene blend by X-ray diffraction (XRD) and atomic force microscopy (AFM) respectively showing the improved device performance to be closely linked to polymer morphological enhancement.

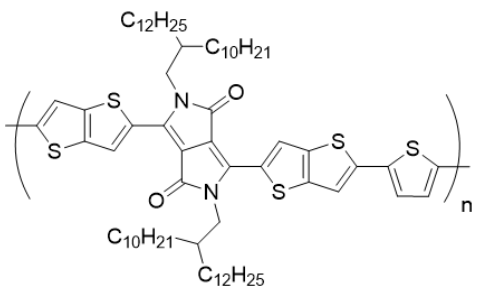

Figure 1. Chemical structure of the previously synthesised $C_{10}C_{12}$DPPTT-T copolymer

Results and Discussion

Polymer fractionation

The $C_{10}C_{12}$DPPTT-T polymer was synthesised by palladium catalysed Stille coupling according to previous literature.[19] The polymer material isolated by Soxhlet extraction in chlorobenzene with no further purification will be referred to as 'non-fractionated' (NF). Following filtration (0.45 µm pore size), the non-fractionated material was fractionated by preparative GPC using chlorobenzene as the eluent and an Agilent PLgel 10 µm MIXED-D column as the stationary phase. During fractionation, the column temperature was maintained at 80˚C to ensure maximum solubility and to reduce aggregation between polymer chains as DPP polymers have previously demonstrated tendencies for aggregation.[2324] The three highest molecular weight fractions (**F1**, **F2** & **F3**) were isolated and re-precipitated into methanol with each of the three purified fractions showing narrowed polydispersity indices compared to the non-fractionated material (Figure 2 and Table 1). The first two fractions **F1** and **F2** have increased molecular weights of M_n 180 kDa and 120 kDa respectively, relative to the non-fractionated material and **F3** shows a reduction with *M*n 80 kDa.

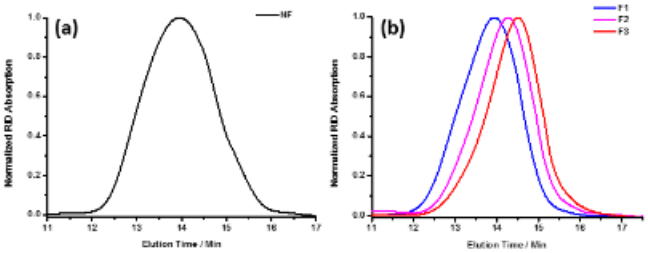

Figure 2. Normalized GPC traces for (a) non-fractionated polymer and (b) purified polymer fractions **F1**, **F2** and **F3**.

Table 1. Polymer physical properties

Polymer	M_n[a] (kDa)	M_w[a] (kDa)	PDI[a]
F1	180	375	2.1
F2	120	220	1.8
F3	80	146	1.8
NF	100	273	2.5

[a] Determined by GPC in chlorobenzene at 80 ˚C with polystyrene standards.

Figure 2 shows normalized polymer GPC traces of non-fractionated material compared to fractions **F1, F2** and **F3**. The original non-normalized elugrams can be found in in the supporting information (ESI). Each elugram shows a normal Gaussian distribution of masses indicative of fully solubilised polymer chains and the effect of the purification is apparent with each fraction being observably narrowed relative to the non-fractionated material.

UVvis spectroscopy

Figure 3 shows the normalized UVvis spectra in both the thin film and solution for non-fractionated, **F1**, **F2** and **F3** materials to evaluate whether the fractionation influences the absorption profile of $C_{10}C_{12}$DPPTT-T polymers. It has been shown that an increase in molecular weight can lead to an increase in

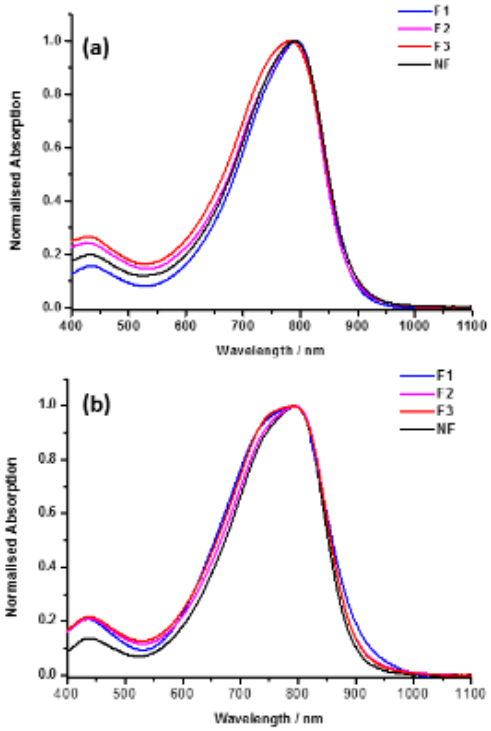

aggregation resulting in a bathochromic shift and/or more pronounced vibronic features

Figure 3 (a) solution (chlorobenzene 25˚C) and (b) thin film (spun from 5 mg / mL chlorobenzene solution) UVvis spectra for non-fractionated, **F1**, **F2** and **F3** materials.

in the absorption profile.[2526] In chlorobenzene solution there is minimal change in absorption between the non-fractionated material and the various molecular weight fractions. There is however a small red shift in absorption maxima that closely follows polymer molecular weight. The absorption maximum for **F3** is at a shorter wavelength (782 nm) in comparison to the non-fractionated material which has a λ_{max} at 789 nm, whilst **F2** and **F1** are more red shifted at 790 nm and 793 nm respectively. It is possible that this is a result of increased aggregation between polymer chains in solution, although such a small shift means that any increase in aggregation is unlikely to be significant. Absorption in the thin film follows the same general trend with the exception of **F2** being slightly more red shifted than **F1**.

OPV device comparison

Bulk heterojunction solar cells with both conventional and inverted device architecture were fabricated using non-fractionated, **F1**, **F2** and **F3** materials as the donor material in the active layers by spin coating of a 1 : 2 polymer / PC[71]BM mixture from chloroform : *o*-dichlorobenzene (4 : 1). The current density vs voltage (*J-V*) curves and external quantum efficiency (EQE) spectra of all four

Table 2. OPV device characteristics with conventional device architecture glass/ITO/PEDOT:PSS/Polymer:PC[71]BM/LiF/Al.

Polymer	J_{sc} (mA cm^{-2})[a]	V_{oc} (V)	Fill Factor	PCE (%)[a]

F1	15.6(±0.6)	0.60(±0.01)	0.67(±0.02)	6.3(±0.3)
F2	14.6(±0.5)	0.61(±0.01)	0.70(±0.01)	6.2(±0.3)
F3	11.2(±0.7)	0.61(±0.01)	0.70(±0.01)	4.8(±0.4)
NF	12.6(±0.5)	0.62(±0.02)	0.53(±0.03)	4.1(±0.3)

[a] EQE corrected. Averaged for 4-5 devices.

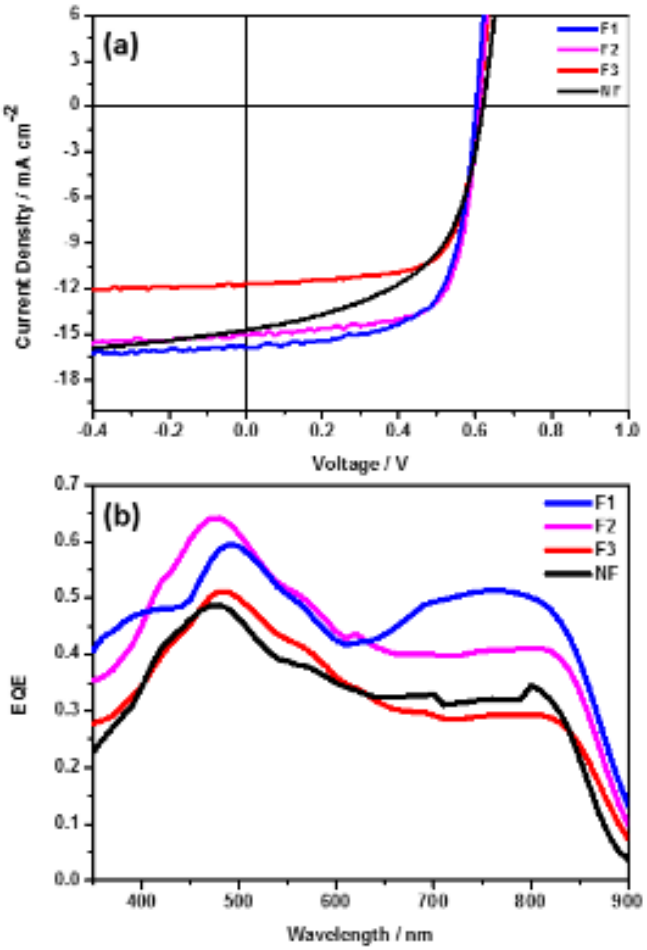

Figure 4. Conventional device architecture (a) Non EQE corrected *J-V* curve for non-fractionated, **F1**, **F2** and **F3** materials (b) External Quantum Efficiency (EQE) spectra for non-fractionated, **F1**, **F2** and **F3** materials**.**

materials are shown for conventional device architecture in **Figure 4** and inverted device architecture in **Figure 5**. The respective device data, corrected for EQE, are summarised in **Tables 2** and **3**. The non-fractionated polymer material demonstrates the lowest overall power conversion efficiency of 4.1 % with a conventional device architecture. An efficiency enhancement up to 4.8 % is observed for **F3** despite it possessing the lowest molecular weight. The enhancement comes from a large increase in fill factor from 0.53 to 0.70. This large increase in fill factor is consistent across all three fractions and it is clear from these results that fractionation is a useful tool towards fill factor enhancement. It is likely that the fill factor enhancement is related to a reduction in lower molecular weight impurities upon fractionation. These impurities can act as charge transport traps and can also impede crystallisation and optimal phase separation. **F2** shows a larger enhancement in efficiency up to 6.2%, in addition to the fill factor enhancement also observed in **F3** there is a significant improvement in J_{sc} with a value of 14.62 mA cm^{-2}.

Of all the device characteristics it appears that J_{sc} is the most sensitive to polymer molecular weight and there is an apparent direct correlation between the two with **F3** showing a drop in photocurrent whilst **F2** and **F1** show an enhancement. **F1** shows similar improvements in device characteristics as **F2** with a PCE of 6.3% as well as a further J_{sc} increase up to 15.58 mA cm^{-2} counterbalanced by a small drop in fill factor to 0.67.

Figure 5 and **Table 3** show the device characteristics when inverted device architecture is employed. The non-fractionated material has a slightly reduced efficiency of 4.0 % compared to devices with conventional architecture. As was observed with the conventional architecture there is minimal variation in V_{oc} across the series. **F3** shows similar improvements as in conventional devices with a reduced J_{sc} and an improved fill factor resulting in a slight increase in overall efficiency. **F2** relative to **F3** shows a large increase in J_{sc} with a value of 14.33 mA cm^{-2} whilst there is a small reduction in fill factor.

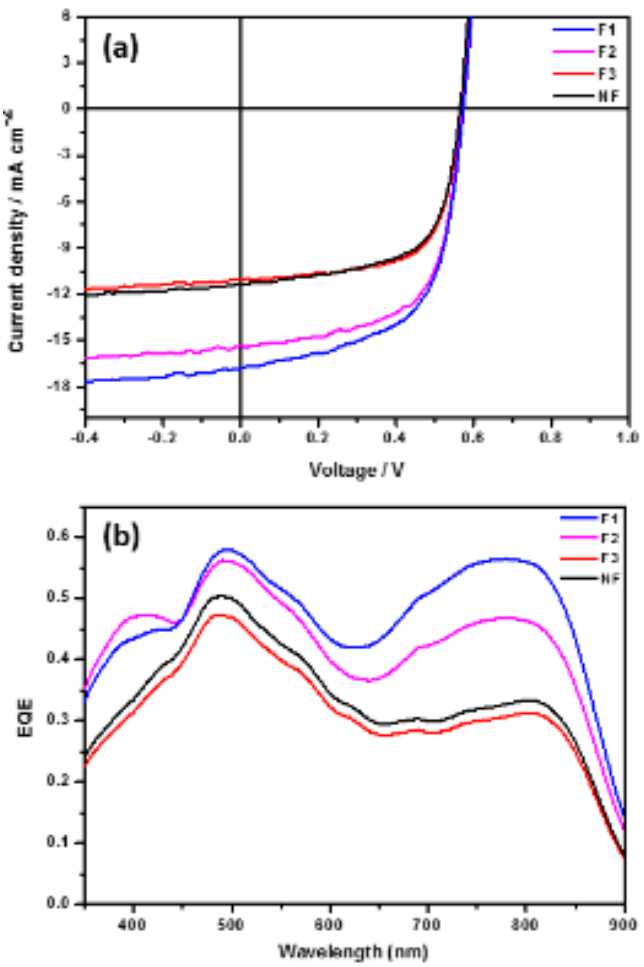

Figure 5. Inverted device architecture (a) Non EQE corrected *J-V* curve for non-fractionated, **F1**, **F2** and **F3** materials and (b) EQE spectra for non-fractionated, **F1**, **F2** and **F3** materials.

Table 3. OPV device characteristics with inverted device architecture glass/ITO/ZnO/Polymer:PC[71]BM/MoO_3/Ag.

Polymer	J_{sc} (mA cm^{-2})[a]	V_{oc} (V)	Fill Factor	PCE (%)[a]
F1	16.0(±0.5)	0.57(±0.01)	0.60(±0.01)	5.5(±0.2)

F2	14.3(±0.3)	0.57(±0.01)	0.64(±0.02)	5.2(±0.3)
F3	10.7(±0.4)	0.57(±0.01)	0.66(±0.01)	4.0(±0.2)
NF	11.4(±0.5)	0.56(±0.01)	0.63(±0.02)	4.0(±0.2)

[a] EQE corrected. Averaged for 4-5 devices.

This translates to a large increase in efficiency from 4.0 % to 5.2% which is further improved to 5.5% in **F1** due to a high J_{sc} of 16.00 mA cm^{-2}. As with conventional architecture the photocurrent closely follows the molecular weight of the materials and overall the trend in efficiency is comparable for both conventional and inverted.

Atomic force microscopy

Charge generation in bulk heterojunction solar cells is known to be closely related to the ability of generated excitons to dissociate.[27] This in turn can be strongly influenced by the intermixing of polymer and fullerene materials with a more intermixed blend morphology allowing a greater number of excitons to reach an interface within the lifetime of the exciton.[2829] Atomic force microscopy (AFM) phase images of the polymer / fullerene blends can be valuable when evaluating the extent of this intermixing and are shown in **Figure 6.** The topography images and corresponding images of the neat polymer films are included in the supporting information (ESI). The non-fractionated material can be seen to have large phase segregation and domain size. In both the conventional and inverted device characteristics this correlates to both the lowest fill factor and overall efficiency. In comparison **F3**, with a lower molecular weight and a narrower polydispersity index can be seen to have reduced phase segregation. Despite the finer intermixing of the

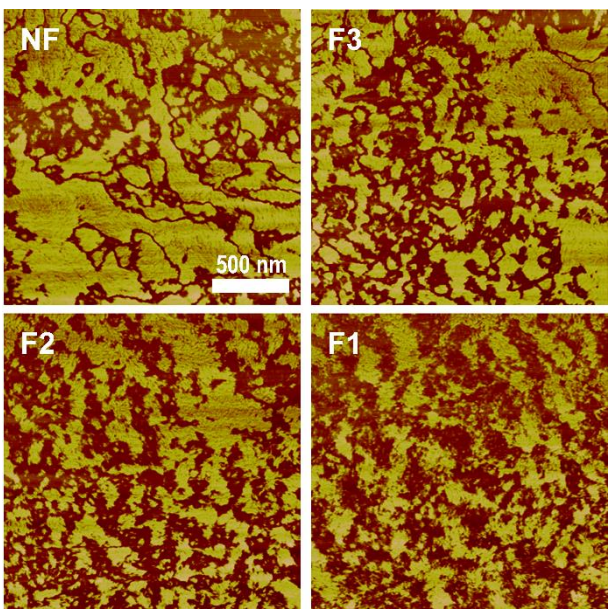

Figure 6. AFM phase images (tapping mode, 2 x 2μm) of polymer / fullerene blends with non-fractionated (**NF**), **F1**, **F2** and **F3** materials spin coated from a chloroform : *o*DCB mixture.

blend in **F3** there can still be seen to be regions of large domain size and as a result the efficiency enhancement remains relatively small for both conventional and inverted devices. **F2** compared to both **F3** and non-fractionated materials sees the disappearance of the large domains. This correlates well with a large increase in efficiency with both sets of devices showing significant enhancement in short circuit currents with inverted and conventional devices giving values of 14.33 mA cm^{-2} and 14.62 mA cm^{-2} respectively. **F1** sees a further improvement in blend morphology and intermixing, which is matched by a further increase in J_{sc} to 16 mA cm^{-2} and a slight decrease in fill factor resulting in slight efficiency improvements in both instances.

X-ray diffraction

Specular X-ray diffraction (XRD) was used to probe drop cast films of the pristine polymer samples. The resultant diffractograms can provide information on the nature and strength of interactions between polymer chains as well as information on the orientation of polymer chains relative to the substrate. **Figure 7** shows XRD diffractions of fractions **F1**, **F2** and **F3** relative to the non-fractionated material. Each of the four materials show an out of plane reflection peak at 2**θ** = ~ 4˚ characteristic of lamellar d spacing (100 peak) which translates to an interlamellar distance of approximately 21.5 Å. This has the lowest intensity for the non-fractionated material whilst the most crystalline is the lowest molecular weight of the three purified fractions **F3**. The two highest molecular weight fractions **F1** and **F2** have intensities about half that of **F3**. This would suggest that there is not a simple relationship between polymer crystallinity and polymer molecular weight or device performance. It has previously been shown that crystallinity is important for the OPV performance of DPPTT-T polymers and it is clear that fractionation induces an increase in crystallinity that influences the device performance likely as a result of a reduction in polydispersity.[30] There is also a smaller crystalline peak at 2**θ** = ~ 8˚ characteristic of second order (200) crystallinity, this peak is indicative of increased crystallinity and is much more pronounced for **F3** which is in agreement with the greater intensity of the **F3** (100) peak.

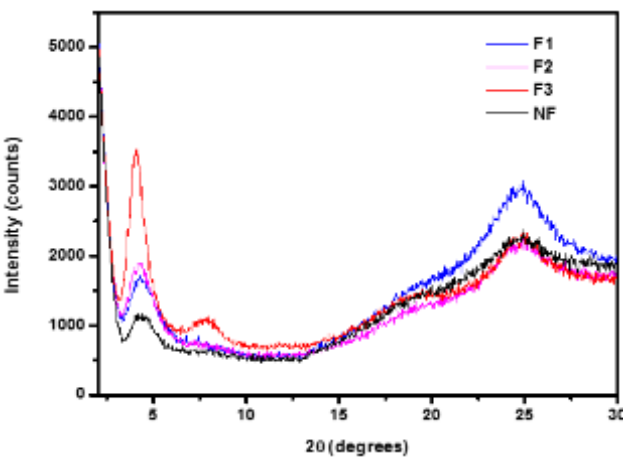

Figure 7. XRD diffractogram of non-fractionated, **F1**, **F2** and **F3** materials. Drop cast from 10 mg / mL chlorobenzene solutions on Si wafers and dried in air overnight.

The low angle diffraction peak at 2**θ** = ~ 25˚ is characteristic of π-π stacking between polymer chains and indicates the presence of chains with a face-on orientation of the backbone plane to the

plane of the substrate. Such an orientation can be favourable for vertical charge transport, a feature that is known to be advantageous for OPV applications. This peak is of similar intensity for non-fractionated, **F2** and **F3** materials but shows a sizeable increase for the highest molecular weight and best performing material **F1**. Furthermore AFM analysis on pristine polymer films (ESI) corroborate the trend in crystallinity observed by XRD, with NF giving the most amorphous surface morphology with a RMS value of 0.94 nm and **F3** affording the roughest surface morphology with a RMS value of 4.34 nm.

Conclusion

Post polymerisation purification and fractionation by preparative gel permeation chromatography is shown to be an effective method in enhancing the power conversion efficiency of $C_{10}C_{12}$DPPTT-T polymer solar cells. Fractionation affords three high molecular weight material fractions with narrowed polydispersities each of which has improved device performance compared to the original material. Performance enhancement is seen to originate from a combination of fill factor and photocurrent improvement with photocurrent values closely following the molecular weight of the fractions. This improvement is observable even when fractionation results in a reduction in molecular weight and improvements are found to be closely associated to the morphological arrangement of the polymer chains in both the neat films and the polymer / fullerene blends. Improved intermixing in blend films is observed with fractionation with the highest molecular weight material giving largely improved efficiencies in excess of 6%. Our findings highlight that thorough optimisation of polymer molecular weight is of paramount importance for applications in OPV devices. Importantly, this optimisation should not only be focused on maximising the number average molecular weight (within the window of sufficient solubility and processability) but also on obtaining sufficiently narrow molecular weight distributions.

Acknowledgements

This work was carried out primarily with funding from The Leventis Foundation, EC FP7 Project X10D and CDT.

Notes and references

[a] *Department of Chemistry and Centre for Plastic Electronics, Imperial College London, London, SW7 2AZ, UK.Address, Address, Town, Country. E-mail: i.meager11@imperial.ac.uk*
[b] *Department of Chemistry, University College London, London, WC1H 0AJT, UK*

† Electronic Supplementary Information (ESI) available: General experimental details, solar cell device fabrication, pristine polymer film AFMs, non-normalized polymer GPCs. See DOI: 10.1039/b000000x/

1. L. Dou, J. You, Z. Hong, Z. Xu, G. Li, R. A. Street, and Y. Yang, *Adv. Mater.*, 2013, **25**, 6642.
2. J. You, L. Dou, Z. Hong, G. Li, and Y. Yang, *Prog. Polym. Sci.*, 2013, **38**, 1909.
3. H. M. Heitzer, B. M. Savoie, T. J. Marks, and M. A. Ratner, *Angew. Chemie Int. Ed.*, 2014, **53**, 1.
4. Y. Shin, J. Liu, J. J. Quigley, H. Luo, and X. Lin, *ACS Nano*, 2014, 8, 6089.
5. H. Zhou, L. Yang, and W. You, *Macromolecules*, 2012, **45**, 607.
6. K. R. Graham, C. Cabanetos, J. P. Jahnke, M. N. Idso, A. El Labban, G. O. Ngongang Ndjawa, T. Heumueller, K. Vandewal, A. Salleo, B. F. Chmelka, A. Amassian, P. M. Beaujuge, and M. D. McGehee, *J. Am. Chem. Soc.*, 2014, 136, 9608.
7. P. Espinet and A. M. Echavarren, *Angew. Chemie Int. Ed.*, 2004, **43**, 4704.
8. Z. Bao, W. K. Chan, and L. Yu, *J. Am. Chem. Soc.*, 1995, **117**, 12426.
9. M. P. Nikiforov, B. Lai, W. Chen, S. Chen, R. D. Schaller, J. Strzalka, J. Maser, and S. B. Darling, *Energy Environ. Sci.*, 2013, **6**, 1513.
10. R. C. Coffin, J. Peet, J. Rogers, and G. C. Bazan, *Nat. Chem.*, 2009, **1**, 657.
11. T.-Y. Chu, J. Lu, S. Beaupré, Y. Zhang, J.-R. Pouliot, J. Zhou, A. Najari, M. Leclerc, and Y. Tao, *Adv. Funct. Mater.*, 2012, **22**, 2345.
12. K. H. Hendriks, G. H. L. Heintges, V. S. Gevaerts, M. M. Wienk, and R. A. J. Janssen, *Angew. Chemie Int. Ed.*, 2013, **52**, 8341.
13. A. T. Yiu, P. M. Beaujuge, O. P. Lee, C. H. Woo, M. F. Toney, and J. M. J. Fréchet, *J. Am. Chem. Soc.*, 2011, **134**, 2180.
14. Z. Li, Y. Zhang, S.-W. Tsang, X. Du, J. Zhou, Y. Tao, and J. Ding, *J. Phys. Chem. C*, 2011, **115**, 18002.
15. Q. Peng, Q. Huang, X. Hou, P. Chang, J. Xu, and S. Deng, *Chem. Commun.*, 2012, **48**, 11452.
16. W. Li, A. Furlan, K. H. Hendriks, M. M. Wienk, and R. A. J. Janssen, *J. Am. Chem. Soc.*, 2013, **135**, 5529.
17. H. Bronstein, Z. Chen, R. S. Ashraf, W. Zhang, J. Du, J. R. Durrant, P. S. Tuladhar, K. Song, S. E. Watkins, Y. Geerts, M. M. Wienk, R. A. J. Janssen, T. Anthopoulos, H. Sirringhaus, M. Heeney, and I. McCulloch, *J. Am. Chem. Soc.*, 2011, **133**, 3272.
18. H. Bronstein, E. Collado-Fregoso, A. Hadipour, Y. W. Soon, Z. Huang, S. D. Dimitrov, R. S. Ashraf, B. P. Rand, S. E. Watkins, P. S. Tuladhar, I. Meager, J. R. Durrant, and I. McCulloch, *Adv. Funct. Mater.*, 2013, **23**, 5647.
19. I. Meager, R. S. Ashraf, S. Rossbauer, H. Bronstein, J. E. Donaghey, J. Marshall, B. C. Schroeder, M. Heeney, T. D. Anthopoulos, and I. McCulloch, *Macromolecules*, 2013, **46**, 5961.
20. R. S. Ashraf, B. C. Schroeder, H. A. Bronstein, Z. Huang, S. Thomas, R. J. Kline, C. J. Brabec, P. Rannou, T. D. Anthopoulos, J. R. Durrant, and I. McCulloch, *Adv. Mater.*, 2013, **25**, 2029.
21. W. R. Mateker, J. D. Douglas, C. Cabanetos, I. T. Sachs-Quintana, J. A. Bartelt, E. T. Hoke, A. El Labban, P. M. Beaujuge, J. M. J. Frechet, and M. D. McGehee, *Energy Environ. Sci.*, 2013, **6**, 2529.
22. S. D. Dimitrov, Z. Huang, F. Deledalle, C. B. Nielsen, B. C. Schroeder, R. S. Ashraf, S. Shoaee, I. McCulloch, and J. R. Durrant, *Energy Environ. Sci.*, 2014, **7**, 1037.
23. M. Kirkus, L. Wang, S. Mothy, D. Beljonne, J. Cornil, R. A. J. Janssen, and S. C. J. Meskers, *J. Phys. Chem. A*, 2012, **116**, 7927..
24. J. Gao, W. Chen, L. Dou, C.-C. Chen, W.-H. Chang, Y. Liu, G. Li, and Y. Yang, *Adv. Mater.*, 2014, **26**, 3142.
25. J. A. Bartelt, J. D. Douglas, W. R. Mateker, A. El Labban, C. J. Tassone, M. F. Toney, J. M. J. Fréchet, P. M. Beaujuge, and M. D. McGehee, *Adv. Energy Mater.*, 2014, **4**, 1301733.
26. D. Wang, Y. Yuan, Y. Mardiyati, C. Bubeck, and K. Koynov, *Macromolecules*, 2013, **46**, 6217.
27. H. Hoppe and N. S. Sariciftci, *J. Mater. Chem.*, 2006, **16**, 45.
28. C. J. Brabec, M. Heeney, I. McCulloch, and J. Nelson, *Chem. Soc. Rev.*, 2011, **40**, 1185.
29. J. Razzell-Hollis, W. C. Tsoi, and J.-S. Kim, *J. Mater. Chem. C*, 2013, **1**, 6235.
30. I. Meager, R. S. Ashraf, S. Mollinger, B. C. Schroeder, H. Bronstein, D. Beatrup, M. S. Vezie, T. Kirchartz, A. Salleo, J. Nelson, and I. McCulloch, *J. Am. Chem. Soc.*, 2013, **135**, 11537.

Table of contents entry

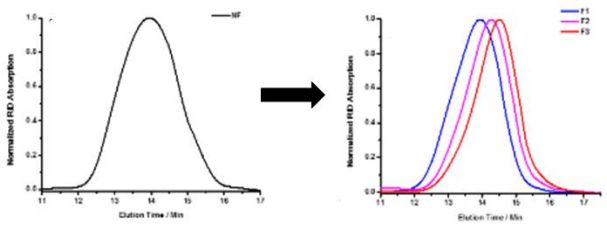

Fractionation of a DPP copolymer by preparative GPC and device optimisation affords signficant organic solar sell performance enhancement